



Study of acid–base properties of supported heteropoly acids in the reactions of secondary alcohols dehydration



J.G. Hernández-Cortez^{a,*}, Ma. Manríquez^b, L. Lartundo-Rojas^c, E. López-Salinas^a

^a Programa de Ingeniería Molecular, Instituto Mexicano del Petróleo, Eje Central Lázaro Cárdenas 152, A.P. 14-805, 07730 Mexico, D.F., Mexico

^b ESIQIE, Instituto Politécnico Nacional, Unidad Profesional "Adolfo López Mateos", Zatzenco, Del. Gustavo A. Madero, 07738 Mexico, D.F., Mexico

^c Centro de Nanociencia y Nanotecnología, Instituto Politécnico Nacional, Unidad Profesional "Adolfo López Mateos", Zatzenco, Del. Gustavo A. Madero, 07738 Mexico, D.F., Mexico

ARTICLE INFO

Article history:

Received 1 April 2013

Received in revised form 4 September 2013

Accepted 6 September 2013

Available online 7 October 2013

Keywords:

Heteropoly acids supported

Dehydration secondary alcohols

DIPE

MIBK

Olefins and ether production

ABSTRACT

The dehydration of secondary alcohols (propan-2-ol and 4-methylpentan-2-ol) was catalyzed by heteropolyacids (HPAs) supported on different solids. Catalysts prepared with 20 wt.% of HPAs were calcined at 400 °C and characterized by X-ray diffraction, Raman spectroscopy, XPS and N₂ adsorption measurements. Stability of the Keggin structure of supported HPAs and changes in textural properties of catalysts were analyzed. The catalytic conversion of alcohols to olefins and ethers has been studied over the catalysts prepared. All catalysts presented activity in the reactions, but only molybdophosphoric acid supported on ZrO₂ (MoP-Z) showed selectivity in the formation of acetone and methyl isobutyl-ketone (MIBK). Catalysts with tungstosilicic acid (WSi) and Tungstophosphoric acid (WP) were active in the formation to DIPE. The acid–base properties of the catalysts play a key role in route of the reaction mechanism.

© 2013 Elsevier B.V. All rights reserved.

1. Introduction

The acidity and basicity of solid catalysts are two influential factors in their activity and selectivity, not only in typical acid–base reactions, different authors reported on the importance of acid–base pair site in many catalytic processes [1,2]. The acid–base properties of the solids are involved in the catalysis of the dehydration reaction producing olefins and ethers that can be accompanied too by alcohol dehydrogenation to the corresponding ketone. Indications as to an application can be found in the patent literature: secondary alcohols were reported to give α-alkenes over thorium and cerium oxides supported on alumina [3] and zirconium oxide catalysts were found to be very selective toward alk-1-ene formation [4,5]. Ether synthesis from alcohol is known to be an acid catalyzed reaction; however, one of the undesirable products is hydrocarbons. Extensive studies on methanol dehydration, mainly over Al₂O₃, have been carried out to address the reaction mechanism. Knözinger and co-workers [6] have proposed that the ether formation takes place via a surface reaction between the adsorbed alcohol molecule on an acidic site and an adsorbed alkoxide anion on a basic site. Other authors have suggested that a Lewis acid–basic pair is responsible for ether formation [7].

4-Methylpent-1-ene is the starting material for manufacturing thermoplastic polymers of interest for their technological properties. This valuable alkene can be prepared through the dehydration of 4-methylpentan-2-ol. The acid–base properties of the solid are evaluated in the dehydration reaction, which can be accompanied by alcohol dehydrogenation to the corresponding ketone.

Heteropolyacids (HPAs) constitute an alternative for the dehydration reactions and others, as they are characterized by a strong acidity, fundamentally of the Brønsted type, comparable to that of fluorhydric and sulfuric acids; some of the more interesting HPAs show the Keggin structure. The Keggin HPAs comprise heteropoly anions of the formula [XM₁₂O₄₀]ⁿ⁻, where X is the heteroatom (P⁵⁺, Si⁴⁺, etc.) and M the addendum atom (Mo⁶⁺, W⁶⁺, etc.). The structure of the heteropoly anion is composed of a central tetrahedron XO₄ surrounded by 12 edge- and corner-sharing metal–oxygen octahedra MO₆ [8]. The HPAs are the usual catalyst of choice because of their acidic strength and relative thermal stability. A serious problem associated with the use of this type of materials as heterogeneous catalysts is their low surface area (~5–8 m² g⁻¹) [9]. The use of HPA in supported form is preferable because of its high surface area compared to the bulk material. Acidic or neutral solids, which interact weakly with HPAs such as silica, active carbon and acidic ion-exchange resin, have been reported to be suitable as HPA supports [10]. Bielánski et al. reported tertiary ether synthesis using WSi on different supports as catalysts [11]. Recently, we had shown that zirconia-supported WP acts as an efficient catalyst for isomerization reaction [12,13].

* Corresponding author. Tel.: +52 55 9175 8409.

E-mail address: jhcortezi@imp.mx (J.G. Hernández-Cortez).

Tungstophosphoric acid ($H_3PW_{12}O_{40}$), tungstosilicic acid ($H_3SiW_{12}O_{40}$) and molibdophosphoric acid ($H_3PMo_{12}O_{40}$) are the most representative of the family of heteropoly acids (HPAs), and their structure is Keggin type [14]. These compounds show high catalytic activity as much in acid–base reactions and oxide–reduction. On the other hand, the HPAs have other special properties, which are very useful in catalysis, such as high solubility in water and in some polar organic solvents, a high thermal stability in solid state and ability to form pseudo-liquid phases. All these properties make possible their use in homogeneous and heterogeneous catalysis [15,16].

The objective of the present study is the evaluation of various solid acid catalysts for alcohols dehydration, mainly 4-methylpentan-2-ol and propan-2-ol. A correlation between catalytic activity and the acid–base properties of the catalysts were investigated.

2. Experimental

2.1. Preparation of catalysts

SiO_2 -Gel (Merk-7734), ZrO_2/SiO_2 (Grace 18301-14 with 13 wt.% of ZrO_2), ZrO_2 (prepared in laboratory by precipitation pH = 10) [12,17] and ZrO_2 thermal treatment at 400 °C (Z^*) for 4 h is used as support. These supports are referred like S, ZS, Z and Z^* , respectively. The HPAs are supported by the impregnation method by the following way: First, solutions of HPAs/ethanol are prepared. Later, the necessary volume of these solutions is added in the different supports, to obtain 20 wt.% of HPAs, the solvent is evaporated using a rotavapor. Finally, the catalysts are dried at 120 °C and calcined at 400 °C for 4 h. The prepared catalysts were denoted as $X-Y$, where X is the corresponding HPA (WP, MoP or WSi) and Y is for S, ZS, Z and Z^* , respectively.

2.2. Characterization of catalysts

The specific surface area, pore volume and pore size distribution of the samples were measured in an automatic adsorption instrument (Quantachrome Autosorb 1C) using low-temperature N_2 adsorption–desorption isotherms. Prior to the measurements, the samples were evacuated in situ at 300 °C for 3 h under vacuum. The surface area was calculated from these isotherms using the multi-point Brunauer–Emmett–Teller (BET) method based on the adsorption data within the partial pressure P/P_0 range from 0.05 to 0.35. The pore size distribution was determined by BJH method from the desorption part of isotherm, the pore volume was determined from total volume of nitrogen adsorbed at $P/P_0 = 0.98–0.99$. All the diffraction patterns (XRD) of the samples were obtained with an Siemens D 5005 apparatus equipped with monochromator of secondary beam for K-radiation $\alpha = 1,5406 \text{ \AA}$ (anode of Cu). Raman spectra were recorded at room temperature on previously calcined samples in a nearly backscattering geometry using an ISA Labram micro-Raman apparatus. The excitation line was the 632.8 nm of a He-Ne laser. The laser power on the sample was kept low (about 1 mW) to avoid thermal effects. The samples were analyzed by X-ray Photoelectron Spectroscopy (XPS), the spectra were acquired with a THERMO Scientific K-Alpha spectrometer equipped with Al $K\alpha$ X-ray source (1486.6 eV) and a hemispherical electron analyzer. Experimental peaks were decomposed into components using mixed Gaussian–Lorentzian functions and a non-linear squares fitting algorithm. Shirley background subtraction was applied. An intensity ratio of 2:3 and a splitting of 2.3 eV were used to fit the Mo 3d peaks. Binding energies were reproducible to within ± 0.2 eV and the C 1s peak at 284.6 eV was used as a reference from carbon.

Table 1
Surface area, pore volume and pore diameter of the different solids.

Sample	S_{BET} ($m^2 g^{-1}$)	Pore volume ($cm^3 g^{-1}$)	Average pore diameter (Å)
Z	204	0.24	47
Z^*	132	0.29	69
S	220	1.05	191
ZS	207	0.95	184
MoP-Z	229	0.22	40
MoP- Z^*	77	0.16	83
WP-S	227	0.86	151
WP-Z	272	0.22	32
WSi-Z	n.e.	n.e.	n.e.
WP-ZS	n.e.	n.e.	n.e.

n.e.=not evaluated.

Z^* stands for ZrO_2 calcined at 400 °C.

2.3. Activity test of catalysts

The catalytic activity of solids was evaluated on the reactions of dehydration of secondary alcohols (4-methylpentan-2-ol and propan-2-ol), these reactions were carried out in a fix-bed quartz tubular reactor. Previous to the reactions, the catalyst was activated at 350 °C with He flow (40 ml/min) during 1 h. On the propan-2-ol dehydration, 0.1 g of sample was used with 60 ml/min He flow as carrier gas (molar ration of He/propan-2-ol = 5). Dehydration of 4-methylpentan-2-ol was carried out with 0.05 g of catalyst and 165 ml/min He flow as carrier gas (molar ration of He/4-methylpentan-2-ol is 39). The products of the reactions were analyzed with a gas chromatograph Varian 3600 CX, connected to the outlet of the reactor and equipped with a Flame Ionization Detector (FID) and PONA capillary column. The reaction rate and conversion were calculated assuming a first order reaction. The following parameters were calculated as follows:

$$X_a \text{ (Conversion of secondary alcohol, mol\%)} = \frac{\sum_i^n Y_i}{C_{out} + \sum_i^n Y_i} \times 100,$$

Selectivity S_i to compound i:

$$S_i \text{ (mol\%)} = \frac{Y_i}{\sum_i^n Y_i} \times 100,$$

where C_{out} is secondary alcohol mole percent in the outlet of reactor and Y_i are yields to the different products.

For a reaction of the type: A → products.

The reaction rate ($-r_a$) was determined using the following equation:

$$-r_a = \frac{F_{ao} X_a}{m}$$

where $-r_a$ = reaction rate [$\text{mol g}^{-1} \text{s}^{-1}$]; F_{ao} = molar flow of A [mol s^{-1}]; X_a = Conversion of A; and m = catalyst mass [g].

3. Results and discussion

3.1. Physico-chemical characterization

In Table 1, the effects caused by the addition of the HPAs on the different supports on the specific area, pore volume and pore average diameter are shown. The ZrO_2 calcined at 400 °C (Z^*), shows a surface area of $132 \text{ m}^2 \text{ g}^{-1}$. When Z was calcined at 300 °C, the area was $204 \text{ m}^2 \text{ g}^{-1}$. The reduction of area is due to the structural transformation by the effect of temperature. The presence of the HPAs produces a stabilization of the area in the supports. The SiO_2 (S) showed a high surface area of $220 \text{ m}^2 \text{ g}^{-1}$ and pore volume of $1.05 \text{ cm}^3 \text{ g}^{-1}$, when the support was impregnated with 20 wt % of WP, the surface area increases to $227 \text{ m}^2 \text{ g}^{-1}$. Similar effect happened with the samples WP-Z and MoP-Z, with areas of 272 and

229 cm² g⁻¹, respectively. The pore volume and average diameter diminished when HPAs were impregnated on the supports; this is because Keggin unit has 12 Å [18] of diameter and its location in the pores of the supports produces a decrease in the volume and diameter of the pores. However, in MoP-Z*, the surface area was very low when MoP was supported on a previously calcined ZrO₂ at 400 °C (Z*), this also affects the pore volume and pore diameter. The samples WSi-Z and WP-ZS were not evaluated in textural properties, however, we have reported that the addition of WP or MoP on ZrO₂ stabilizes the surface area of the resulting solid acid in comparison with that of pure ZrO₂ [12,19], so we expect a similar behavior in the stabilization of the area of the WSi-Z and WP-ZS samples.

Kozhevnikov reported that the thermal stability of HPAs has the following order PW > SiW > MoP [28] and above of 450 °C, the Keggin structure of H₃PMo₁₂O₄₀ is completely destroyed [27]. In the Figs. 1 and 2, XRD patterns of supports, pure HPAs and the solids with a content of 20 wt.% of HPAs, within 2θ range of 4–70° are shown. The XRD of pure HPAs (dried at 120 °C) showed large number of narrow peaks, being the characteristic pattern of a crystalline structure type body-centered cubic [20]. The Z (ZrO₂) and ZS showed a broad peak, extending from 15 to 40° 2θ range, which indicated that the supports are present in the amorphous state. In patterns of the samples, MoP-Z, WP-Z and WSi-Z, recorded after calcining at 400 °C, a portion of the amorphous material crystallizes into tetragonal ZrO₂ showing no indication of any crystalline phases related to HPAs. The reason of these results may be that HPAs particles are too small and/or too well dispersed and therefore undetectable by XRD. However, in samples WP-S and WSi-S characteristic peaks related to the HPAs were detected. These results suggest a strong interaction between HPAs particles and ZrO₂ surface, either in the hydrated or stabilized state. In the sample MoP-Z*, all the amorphous material crystallizes into tetragonal and monoclinic ZrO₂, without detecting any crystalline phase related to MoP. This good dispersion can be due to the mean pore diameter of the supports which is bigger at 30 Å (see Table 1) while the diameter of the HPA is about 12 Å [18]. This difference in the pore diameter can allow a more uniform distribution of HPAs on the supports surface, minimizing the possibility of agglomerations which could induce crystallization. Recently, we reported that the collapse of the WP Keggin structure occurs at temperatures above 500 °C, which yields WO₃ and phosphates [17]. A comparison between the XRD patterns of 20 wt % WP or WSi loaded on Z and S indicates that the interaction of HPA with S is much weaker than that with Z.

The Raman spectrum of MoP-S (see Fig. 3) under ambient conditions exhibits the characteristic bands of the Keggin structure. The relative intensities of the Raman bands due to Mo—O vibrations at 839, 673, and 234 cm⁻¹, are assigned to the symmetric/antisymmetric stretching modes of terminal and bridging Mo—O, and their bending vibrations, respectively. The band at 234 cm⁻¹ corresponds to the bridging Mo—O—Mo bending modes of the intact Keggin. A pronounced shift of the Mo=O bands are observed from the band to 839 and 994 cm⁻¹ of crystalline MoO₃ and at 673 cm⁻¹ band result of the three-bridged oxygen stretching motion. The bands to 821 and 1006 cm⁻¹ correspond of crystalline MoO [21–23]. PO₄ species, present a symmetric stretching mode to 1071 cm⁻¹ (spectrum Fig. 3) and finally the band at 342 cm⁻¹ indicate the formation of a polyoxoanion with the Keggin structure.

The Raman spectrum of sample MoP-ZS is shown in Fig. 3. The main bands characteristic of the Keggin heteropolyanion (MoP) are 1006, 995, 920–896, 800, 620, and 245–214 cm⁻¹, related, respectively, to stretching modes $\nu_s(\text{Mo}=\text{O}_t)$, $\nu_{as}(\text{Mo}=\text{O}_t)$, $\nu_s(\text{Mo}=\text{O}_b-\text{Mo})$, $\nu_s(\text{Mo}-\text{O}_c-\text{Mo})$ and $\nu_s(\text{Mo}-\text{O}_a)$ [24]. A pronounced shift of the Mo=O band from 817 and 992 cm⁻¹ observed bands of crystalline MoO₃ the symmetric stretching mode and that at 1156 cm⁻¹ of PO₄ species. Raman bands at 113, 124,

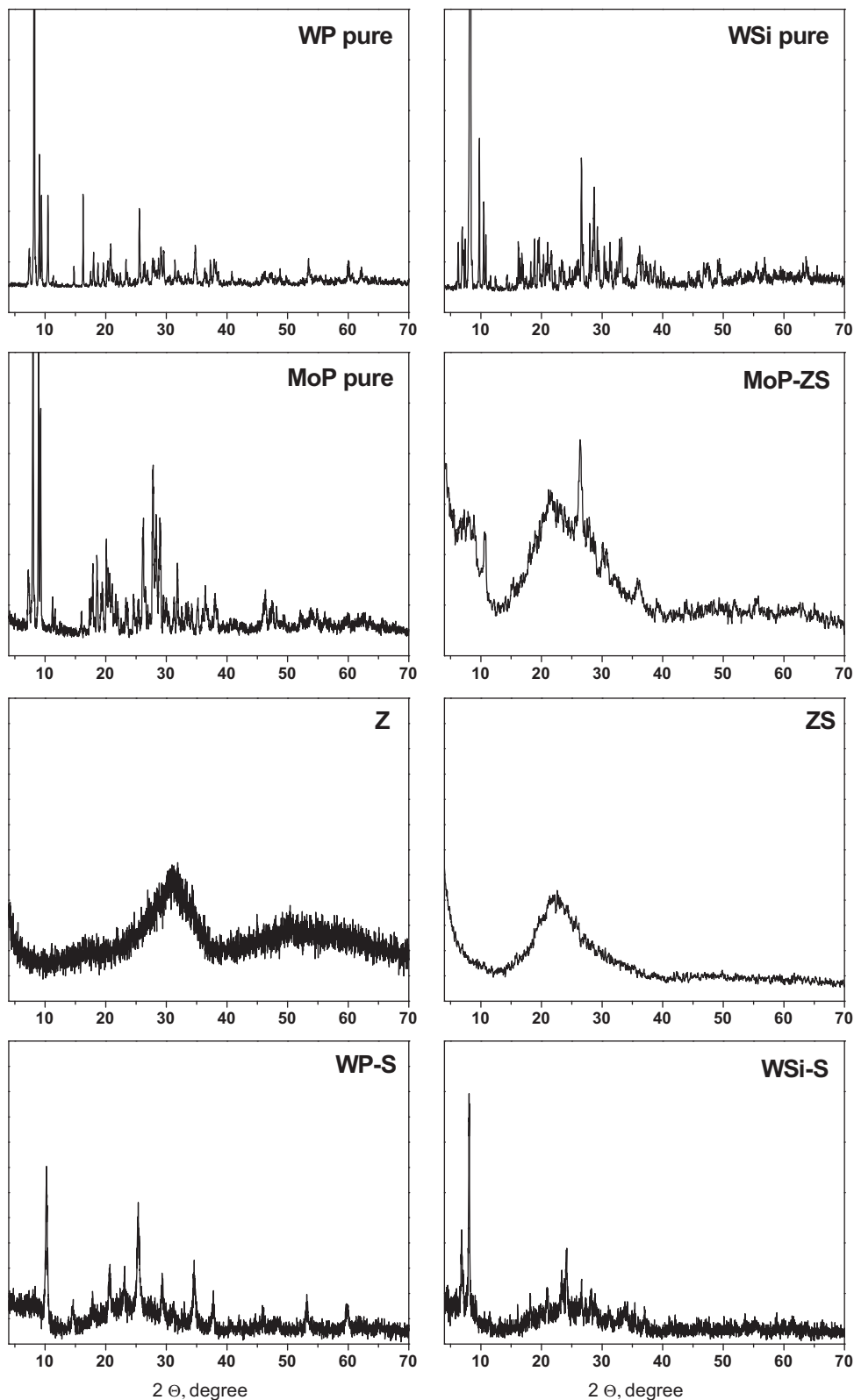
153, and two small bands to 198 and 218 cm⁻¹ corresponding to tetragonal phase zirconium [25,26]. The Raman bands assigned to Mo—O vibrations at 234 cm⁻¹, these bands are assigned to the symmetric/antisymmetric stretching modes of terminal Mo—O groups. Finally, two bands are also observed at 375 and 335 cm⁻¹, which is typical of the Keggin structure [22,26], indicating that molybdophosphoric acid was not decomposed upon calcinations at 400 °C. However, when MoP is supported on a hydrated zirconia, containing abundant OH groups (MoP-Z), the characteristic peaks of MoP are not observed, suggesting its high dispersion [12]. Assuming this, a strong interaction between surface Zr—OH groups and MoP framework oxygens may be taking place, particularly with terminal oxo Mo=O bonds.

Raman spectra of WSi-ZS and WSi-S are presented in the same Fig. 3. The Raman bands can be attributed to Keggin structure, in accordance with the literature [27–29]. In WSi-ZS sample, Raman bands from 119 to 205 cm⁻¹ correspond to tetragonal zirconium. Assignments of the observed bands are as follows, two strong bands of 1003 and 803 cm⁻¹ attributed to symmetric and asymmetric stretching (W—O), respectively. The Raman band at 1062 cm⁻¹ attributed to symmetric stretching of the tungsten-terminal oxygen (W=O) within WO₆ octahedral. Weak bands are also observed at 784 and 534 cm⁻¹ attributed to (W—O—W), see WSi-S sample. The bands at 235 y 269 cm⁻¹ corresponds to the bridging W—O—W bending modes of the intact Keggin structure.

Fig. 4 shows XPS spectra of the W 4f of the sample WSi-S. The presence of two shoulders besides the main doublet are observed. This spectrum was fitted with three different doublets of W 4f with 4f_{7/2} located at 33.6, 34.2, 34.6 and 38.0 eV. The major contribution is from the first peak. The samples show only one form of W having 4f_{7/2} binding energy at 38.0 eV. Therefore, the peaks 33.6, 34.2 and 38.0 eV peaks are related to the presence of water on the sample surface, the peak a 34.6 eV is assigned to interaction of phosphorus species with WO₃. The signals at 33.6 eV correspond to reduced species of WO₂ and W—O—W. The signal at 38.0 eV corresponds to species of WO₃. Oxygen (O 1s) presents the following contribution in the sample WSi-ZS (see Fig. 4). At 531 eV is assigned the interaction of Oxygen with ZrO₂, at 530 eV shows the interaction of oxygen with WO₃ species, already 528 eV is assigned O—O species, it is observed the interaction of oxygen with the W species in its reduced state as WO₂. At 532.27 eV the oxygen interaction with SiO₂ species, and finally to 529 eV are observed OH on the surface [23,30,31]. The XP spectra of the ZrO₂ used as support in the sample WSi-Z are shown in Fig. 4. The BE of the Zr (3d) photoelectron peaks at 182.31, 184.31 and 185 cm⁻¹. The peak at 184.31 eV corresponds to interaction HPA with zirconia. The first signal of ZrO₂ (Zr 3d_{5/2}) at 182.31 and the third at 185 eV (Zr 3d_{3/2}) are related to the presence of water on the sample surface of ZrO₂ [32,33]. This information provides evidence of the presence of one type of ZrO₂ with an oxidation state of +4. The values of peaks for Mo 3d core level at 228.38–233.08 suggest the presence of Mo (VI) in polymolybdates species [34,35]. The value observed to 233.08 eV suggests the presence of molybdenum in the oxidation states of MO₃ that correspond to higher binding energies of Mo 3d_{5/2}. The peaks at 228.38 and 230.0 eV were assigned to Mo (V) species, accordingly energy binding value to Mo3d_{5/2}, is due to reduced molybdenum species of MoO₂ [36]. The other peak at 231.41 eV corresponds to MoO_x species [37]. This spectrum shows clearly the presence of reduced molybdenum.

3.2. Activity test of catalysts

In order to examine the catalytic activity of the supported HPAs, the catalysts were evaluated in the decomposition of propan-2-ol (Table 2). This reaction has been extensively reported as a valuable catalytic test to analyze the acid–basic properties of heterogeneous

**Fig. 1.** XRD patterns of pure HPA's, supports and HPA-S samples.

catalysts [38]. Pure MoP only showed activity at 200 °C, this HPA presented a conversion of 21.2 mol% and its selectivity was: propylene (87.2 mol%), acetone (8.8 mol%) and DIPE (4 mol%). The HPAs supported on ZrO₂ presented more catalytic activity than pure ZrO₂. The selectivity is oriented mainly toward the formation of

propylene and as reaction by-product to di-isopropyl ether (DIPE). It is important to notice that the DIPE formation is a potential additive to increase the octane in reformulated gasoline. On the other hand, the catalyst with lower activity is MoP-Z. Nevertheless, this solid besides dehydrating the alcohol, presented oxidant

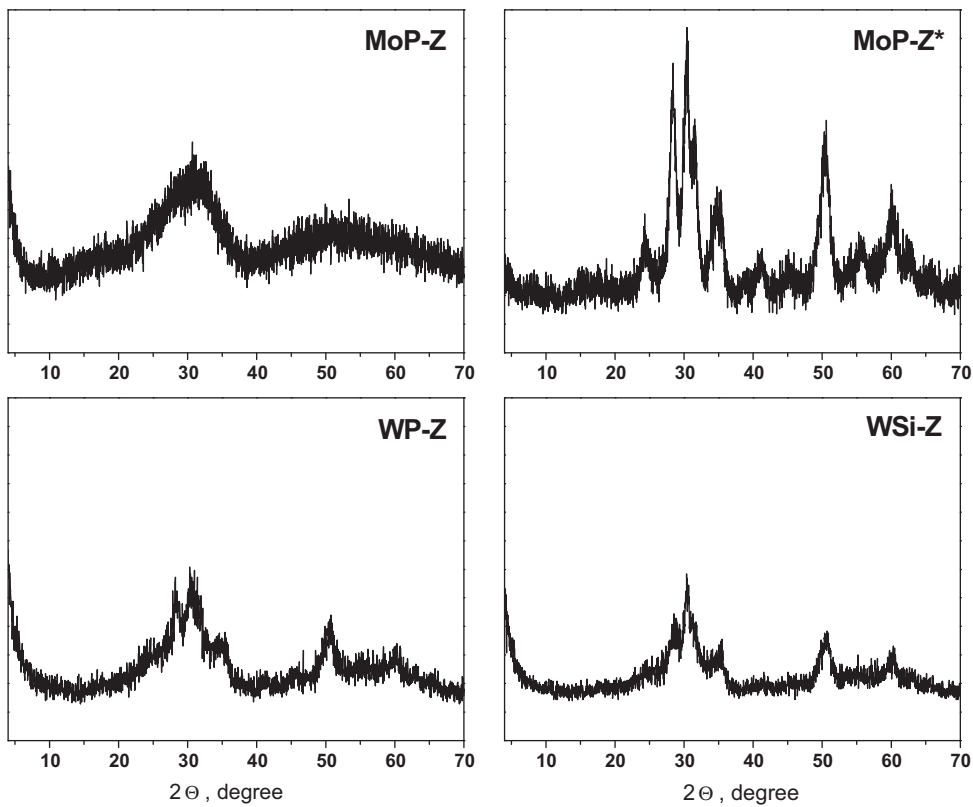


Fig. 2. XRD patterns of HPA-Z samples.

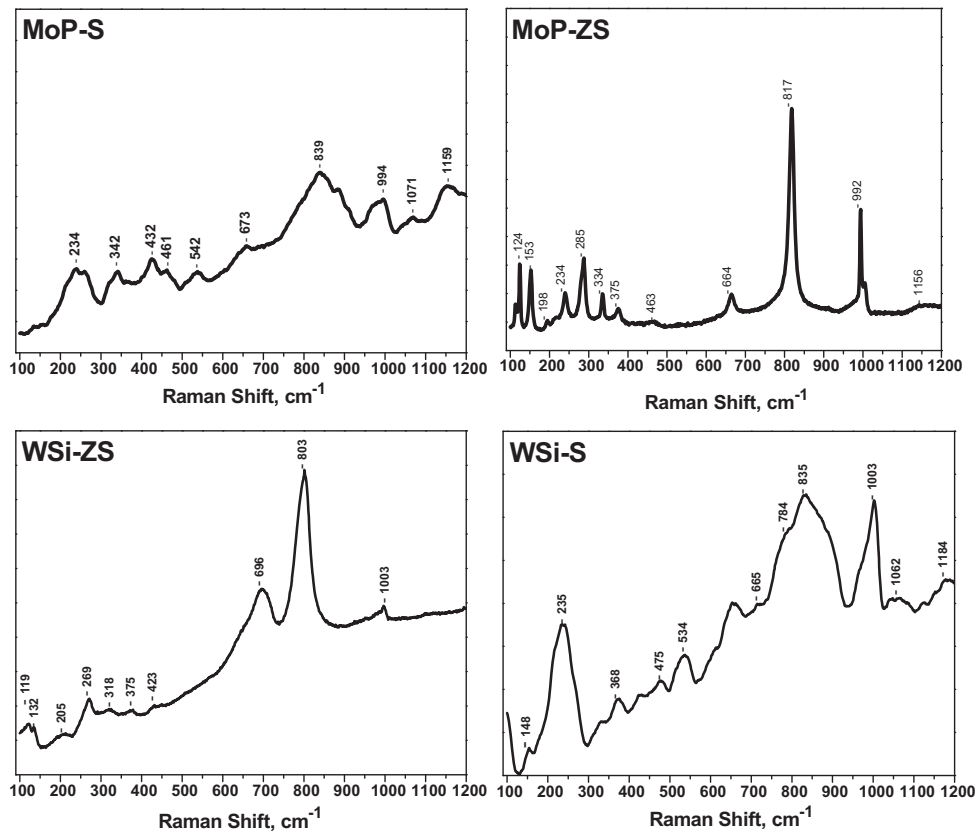


Fig. 3. Raman spectra of the different catalysts.

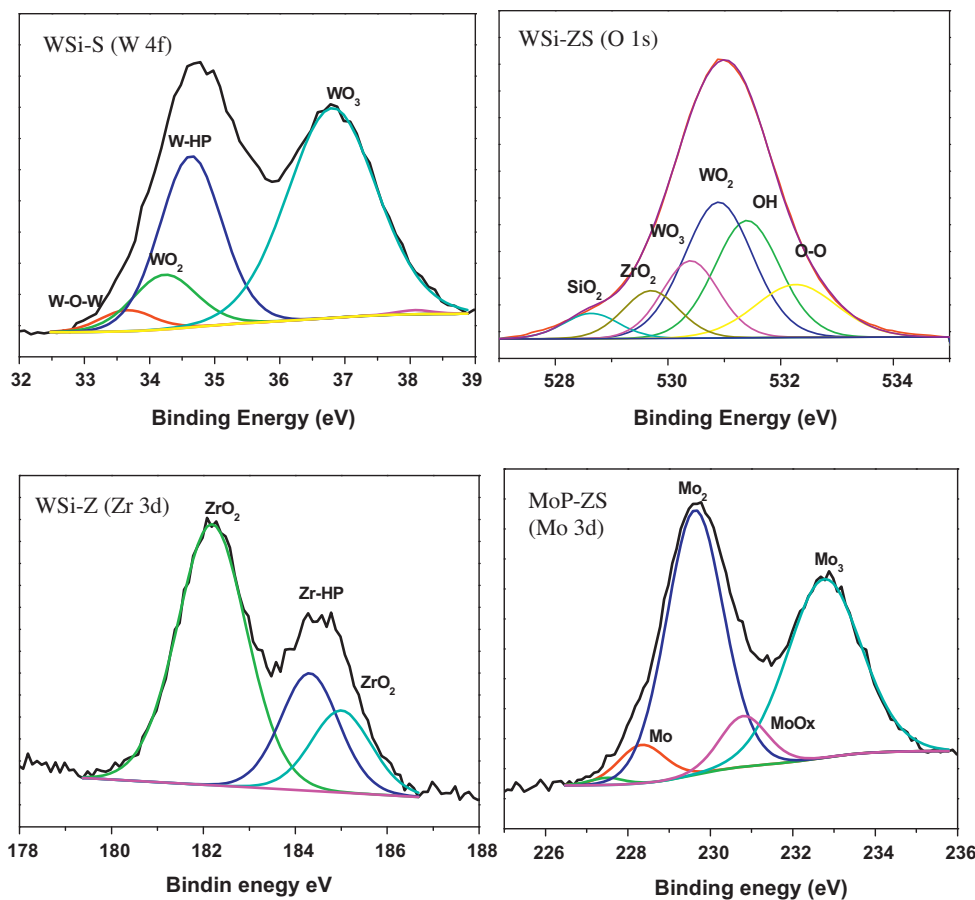


Fig. 4. X-ray photoelectron spectra of: O 1s, Mo 3d, W 4f and Zr 3d.

Table 2
Conversion, reaction rates and selectivity in the reaction of propan-2-ol at 175 °C.

Catalyst	Conversion ^a (mol%)	Selectivity (mol%)	$-r_a \times 10^{-4}$ (mol/g min)
	Propylene	Acetone	DIPE
Z ^b	1.4	100	0
MoP ^b	21.2	87	4
WP-Z	29.9	80	20
WSi-Z	51.2	86	14
MoP-Z	22.2	95	0

^a Taken after 15 min of reaction.

^b Reaction at 200 °C.

Table 3
Conversion, reaction rates and selectivity in the reaction of propan-2-ol at 115 °C.

Catalyst	Conversion ^a (mol%)	Selectivity (mol%)			$-r_a \times 10^{-5}$ (mol/g min)
		Propylene	Acetone	DIPE	
MoP-Z	2.3	42.7	15.5	41.9	8.7
WSi-Z	1.6	41.8	0.0	58.2	6.0
WSi-Z*	5.0	47.2	0.0	52.8	19.4
WP-Z	1.6	38.0	0.0	62.0	6.3
WP-Z*	4.8	55.7	44.3	0.0	14.1
WP-S	4.9	85.4	0.0	14.6	8.1

Z* stands for ZrO₂ calcined at 400 °C.

^a Taken after 15 min of reaction.

properties because of Mo, which not only orients selectively toward the dehydration of the alcohol, but also toward the formation of acetone. The reaction rate is influenced by the type of HPA supported; WSi-Z and WP-Z catalysts had greater reaction rate of 19.8 and 11.6 mol/g min, respectively.

The results of the catalytic evaluation at 115 °C are presented in Table 3. The supports used in this study do not present activity in the decomposition of propan-2-ol at this temperature. When HPAs were deposited on the supports an increment was observed in activity, which depends on the interaction of the HPAs with the supports and the generation of acid sites [16]. We reported that the impregnation of WP on Z yields strong solid acids ($H_o \leq -9.3$, calcined at 400 °C), the sites are predominantly Lewis acids when WP was supported on hydrated ZrO₂ and then calcined at 400 °C, but both Bronsted and Lewis acid sites are observed when WP was supported on a previously calcined zirconia (Z*) or with SiO₂ (S) [12]. The WP-S, WP-Z* and WSi-Z* catalysts showed the major conversion of propan-2-ol with values of 4.9, 4.8 and 5.0 mol%, respectively. The high activity of these catalysts is due to the formation or presence of Bronsted acidity. The selectivity is oriented mainly toward the formation of propylene and DIPE. The other catalysts presented a lower conversion of propan-2-ol with the selectivity oriented to the formation of propylene and DIPE. The selectivity for propylene product ($C_3^=$) depended on the acid sites type generated by HPAs on the supports. In the case of MoP-Z the formation of 15.5 mol% of acetone was observed. The basic sites contained in the MoP system reported in the literature [39,40] have an important role in the selectivity to acetone. The basic sites present on the catalysts of MoP-Z favor the selectivity to acetone.

In general it is conventionally accepted that acid sites are the responsible for the dehydration activity yielding propylene. In a similar way, in the production of acetone (dehydrogenated product) acid and basic sites are required. On the other hand, for the formation of the ether only acid sites of moderated strength are involved. Considering our previously reported studies [12,16,17], we can state that dehydration and formation of DIPE takes place

Table 4

Conversion, reaction rates and selectivity in the reaction of 4-methylpentan-2-ol.

Catalyst	Conversion ^a (mol%)	Selectivity (mol%)				$-r_a \times 10^{-5}$ (mol/g min)	
		A	B	C	D		
WP	5.9	12.6	57.5	28.0	1.85	0.0	15.6
WP-S	3.1	15.7	54.7	29.6	0.0	0.0	8.4
WP-ZS	3.1	17.6	47.7	34.7	0.0	0.0	8.4
WP-Z	3.8	13.9	74.6	11.5	0.0	0.0	10.2
WP-Z*	9.0	16.0	75.8	8.2	0.0	0.0	22.8
MoP-Z	18.0	14.1	66.4	10.5	0.0	9.0	41.4
MoP-Z*	22.5	13.5	60.3	20.7	0.0	5.5	52.4

A=1,2 Dehydration; B=cis/trans isomerization; C=double bond migration; D=skeletal isomerization; and MIBK=methyl isobutyl-ketone.

Z* stands for ZrO₂ calcined at 400 °C.

^a Taken after 10 min of reaction. T reaction = 100 °C.

on Bronsted or Lewis acid sites. However, it can be interpreted in view of the relative stability of correspondent carbenium ions, that the reaction occurs between gas-phase and alcohols adsorbed (as carbenium species) species. When the temperature was increased, the amount of adsorbed alcohols species on the surface of the catalysts decreased, consequently the production of DIPE dropped too.

The rate and selectivity for 4-methylpentan-2-ol conversion reactions were determined at 100 °C. The alcohol is converted on calcined samples via two main groups of reactions: dehydration and dehydrogenation. Dehydration of 4-methylpentan-2-ol leads to olefins as predominant products, and the dehydrogenation reaction produce MIBK. The results of the catalytic activity in the reaction of 4-methylpentan-2-ol using the different catalysts are presented in Table 4. The catalysts with greater catalytic activity are MoP-Z* and MoP-Z with 22.5 and 18.0 mol% of conversion of alcohol, respectively. The selectivity is oriented mainly toward the formation of dehydration, cis/trans isomerization and double bond migration products. Nevertheless, MoP-Z also presented the MIBK formation, which indicates the presence of basic properties given to the Mo in this catalyst.

WP-S and WP-ZS showed the lowest conversion of 3.1 mol% and selective to olefins (dehydration, cis/trans isomerization and double bond migration) formation. Pure WP presented better catalytic activity than when it is deposited on the supports of S, ZS and Z. The increase in catalytic activity was observed in MP-Z* catalyst with a conversion of 9 mol% and a reaction rate of 22.8 mol/g min, this activity is due to the presence of Lewis and Bronsted acid sites, which increases the total acidity. When MoP is supported on Z*, the conversion increased slightly, since there is a greater amount of acid sites. This increase in acidity produced a greater selectivity toward products of migration of double bond, in which strong acid sites are required [41]. The ZrO₂ sample has presented null activity at 100 °C. The activity of ZrO₂ at 160 °C was of 8 mol% [42] and pure WP showed conversion of 5.9 mol% and selective to olefins (dehydration, cis/trans isomerization and double bond migration) formation.

4. Conclusions

This paper has shown that a combination of Raman spectroscopy, X-ray photoelectron spectroscopy and X-ray diffraction can be used to perform the characterization of supported HPAs. The interaction between HPAs and supports influences the physicochemical properties of prepared solids. The addition of the HPAs stabilizes the surface area of the resulting solid in comparison with the pure supports. The HPAs retained their Keggin structure when they are supported. The activity of the catalysts in dehydration of

secondary alcohols depends on the type of HPAs used. DIPE production is formed only in catalysts that contain WSi and WP (acid sites of moderated strength are required). The MoP-Z catalyst exhibited mainly acid and base properties given that acetone and MIBK are obtained in dehydration of secondary alcohols. These reactions can be employed to study the acid-base properties of catalysts.

References

- [1] K. Tanabe, Trends Anal. Chem. 13 (1994) 164–168.
- [2] K. Tanabe, T. Yamaguchi, Catal. Today 20 (1994) 185–197.
- [3] C.A. Drake, US Patent 4417089 (1983).
- [4] M. Araki, K., Takahashi, T., Hibi, Eur. Pat. EP0150832 (1985).
- [5] M. Araki, T., Hibi, Eur. Pat. EP0222356 (1986).
- [6] H. Knözinger, K. Kochloeft, W. Meye, J. Catal. 28 (1973) 69–75.
- [7] J.E. Dabrowski, J.B. Butt, H. Bliss, J. Catal. 18 (1970) 297–313.
- [8] M.T. Pope, *Heteropoly and Isopoly Oxometalates*, Springer-Verlag, Berlin, 1983.
- [9] J.A. Kocal, B.V. Vora, T. Imai, Appl. Catal. A: Gen. 221 (2001) 295–301.
- [10] Y. Wu, X. Ye, X. Yang, X. Wang, W. Chu, Y. Hu, Ind. Eng. Chem. Res. 35 (1996) 2546–2560.
- [11] A. Bielanska, A. Lubanska, J. Pozniczek, A. Micek-Ilnicka, Appl. Catal. A: Gen. 238 (2003) 239–250.
- [12] E. López-Salinas, J.G. Hernández-Cortez, M.A. Cortes-Jacome, J. Navarrete, M.E. Llanos, A. Vazquez, H. Armendariz, T. López, Appl. Catal. A: Gen. 175 (1998) 43–53.
- [13] W. Kuang, A. Rives, M. Fournier, R. Hubaut, Appl. Catal. A: Gen. 250 (2003) 221–229.
- [14] G.A. Tsigdinos, Top. Curr. Chem. 76 (1978) 1–64.
- [15] K. Tanabe, M. Misono, Y. Ono, H. Hattori, New solid acids and bases, their catalytic properties, Stud. Surf. Sci. Cat. 51 (1989) 163–173.
- [16] J.G. Hernández-Cortez, L. Martinez, L. Soto, A. López, J. Navarrete, Ma. Manríquez, V.H. Lara, E. López-Salinas, Catal. Today 150 (2010) 346–352.
- [17] E. López-Salinas, J.G. Hernández-Cortéz, I. Schifter, E. Torres-García, A. Gutiérrez-Carrillo, T. López, P.P. Lottici, D. Bersani, Appl. Catal. A: Gen. 193 (2000) 215–225.
- [18] I.V. Kozhevnikov, Catal. Rev. Sci. Eng. 37 (1995) 311–352.
- [19] J.G. Hernández-Cortez, E. López-Salinas, Ma. Manríquez, J.A. Toledo, M.A. Cortes-Jacome, Fuel 100 (2012) 144–151.
- [20] Y. Izumi, K. Urabe, M. Onaka, Zeolite, Clay and Heteropoly Acid in Organic Reactions, Kodansha/VCH, Tokyo, 1992, pp. 99–161.
- [21] A. Predoeva, S. Damyanova, E.M. Gaigneaux, L. Petrov, Appl. Catal. A: Gen. 319 (2007) 14–24.
- [22] C. Rocchiccioli-Deltcheff, M. Fournier, R. Franck, R. Thouvenot, Inorg. Chem. 22 (1983) 207–216.
- [23] C. Rocchiccioli-Deltcheff, R. Thouvenot, R. Frank, Spectrochim. Acta 32A (1976) 587.
- [24] G. Mestl, T. Ilkenhans, D. Spielbauer, M. Dieterle, O. Timpe, J. Krohnert, Appl. Catal. A: Gen. 210 (2001) 13–34.
- [25] M. Kilo, C. Schild, A. Wokaum, A. Baiker, J. Chem Soc, Faraday Trans. 88 (1992) 1453–1457.
- [26] P.D.L. Mercera, J.G. Van Ommen, E.B.M. Doesburg, A.J. Burggraaf, J.R.H. Ross, Appl. Catal. 57 (1990) 127–148.
- [27] N. Mizuno, M. Misono, Chem. Rev. 98 (1998) 199–217.
- [28] I.V. Kozhevnikov, Chem. Rev. 98 (1998) 171–198.
- [29] L. Nakka, J.E. Molinari, I.E. Wachs, J. Am. Chem. Soc. 131 (2009) 15544–15554.
- [30] D. Briggs, M.P. Seah, *Practical Surface Analysis and X-ray Photoelectron Spectroscopy*, 2nd ed., Wiley, Chichester, 1990.
- [31] S. Damyanova, J.L.G. Fierro, A. Spojakina, React. Kinet. Catal. Lett. 56 (1995) 321.
- [32] B.M. Reddy, P.M. Sreekanth, Y. Yamada, Q. Xu, T. Kobayashi, Appl. Catal. A: Gen. 228 (2002) 269–278.
- [33] K.V.R. Chary, K.R. Reddy, G. Kishan, J.W. Niemantsverdriet, G. Mestl, J. Catal. 226 (2004) 283–291.
- [34] J.C. Muijsers, Th. Weber, V. van Hardeveld, H.W. Zandbergen, J.W. Niemantsverdriet, J. Catal. 157 (1995) 698–705.
- [35] Th. Weber, J.C. Muijsers, J.H.M.C. van Wolput, C.P.J. Verhagen, J.W. Niemantsverdriet, J. Phys. Chem. 100 (1996) 14144–14150.
- [36] S.M.A.M. Bouwens, J.A.R. van Veen, D.C. Koningsberger, V.H.J. de Beer, R. Prins, J. Phys. Chem. 95 (1991) 123–134.
- [37] A.D. Gandubert, E. Krebs, C. Legens, D. Costa, D. Guillaume, P. Raybaud, Catal. Today 130 (2008) 149–159.
- [38] L.M. Gomez Sainero, S. Damyanova, J.L.G. Fierro, Appl. Catal. A: Gen. 208 (2001) 63–75.
- [39] X.Z. Fu, Z.X. Dong, W.Y. Su, D.Z. Li, J. Catal. 20 (1999) 321.
- [40] R. Gomez, T. Lopez, E. Ortiz-Islas, J. Navarrete, E. Sanchez, F. Tzompantzti, X. Bokhimi, J. Mol. Catal. A: Chem. 193 (2003) 217–226.
- [41] P. Berteau, B. Delmon, J.-L. Dallons, A. Van Gysel, Appl. Catal. 70 (1991) 307–323.
- [42] A. Auroux, P. Artizzu, I. Ferino, V. Solinas, G. Leoanti, M. Padovan, G. Messina, R. Mansani, J. Chem. Soc. Faraday Trans. 91 (1995) 3263–3267.